Predictive Direct Power Control of a Grid Connected Three-Phase Voltage Source Inverter for Photovoltaic Systems

M.N. Amrani*‡, A. Dib*

* Department of Science and Technology, Laboratory LGEA, University of Oum-El-Bouaghi

(amranimednader@yahoo.fr, dibabderrahmane@yahoo.fr)

‡ Corresponding Author; M.N.Amrani, University of Oum-El-Bouaghi amranimednader@yahoo.fr

Abstract- This paper deals with the control of a three-phase voltage source inverter (VSI) for a grid-connected photovoltaic (PV) system. The direct power control (DPC) is combined with a predictive approach for selecting the optimal inverter switching states. This optimal selection is carried out by minimizing a suitable cost function. Moreover, in order to extract the maximum available power from the PV generator, a fuzzy logic maximum power point tracking (MPPT) controller is applied to a DC-DC quadratic boost converter acting as an interface between the PV generator and the inverter. Modelling and simulation of the system were performed by using Matlab/Simulink software

Keywords Grid-Connected PV Systems; Quadratic Boost Converter; Fuzzy Logic Controller; Direct Power Control; Predictive Direct Power Control.

1. Introduction

Solar energy is one of the most promising sources of renewable energies that can be used as an alternative to fossil energy. Among its applications, electricity generation using photovoltaic (PV) panels has been widely considered during the last years due to several advantages [1]. Namely, PV systems are easy to install and require low maintenance efforts [2]. Generally, there are two types of electrical energy generation PV systems namely, autonomous and grid connected systems. The grid connected PV systems consist of PV generators, two power converters and the electrical grid. The first converter is a DC-DC structure connected to the output of the PV generator and it is responsible for maximum power point tracking (MPPT). The second one is a DC-AC inverter which has the role of injecting the harvested energy from the PV generator into the electrical grid.

The voltage and power of a PV generator vary with temperature and irradiance. The maximum output voltage of a PV generator ranges from 15 V to 40 V, which is much smaller compared to the input voltage of the three-phase VSI ranging from 380 V to 400 V, and therefore a high voltage gain converter must be used as a power interface, hence implying the operation of a high duty-cycle value, which is not practical due to the non-ability of reaching high values of voltage gains in the presence of losses. One of the solutions to avoid the use of high duty-cycle values is the serial interconnection of several PV generators to a central power converter with the disadvantages of high sensitivity to mismatch because of the use of a centralized MPPT. As a

remedy, the conventional boost converter may be substituted with a high voltage gain converter that could work with relatively low values of duty-cycle. Several topologies have been developed for PV systems with high voltage gain to ensure sustainable, reliable and efficient use of solar energy in either grid-connected or stand-alone applications. Among others, we can quote switched capacitor and switched inductor converters [3, 4], voltage multipliers and coupled inductor converters [5, 6], cascaded boost converters where each could operate with relatively low values of duty-ratio [7–9]. However, all these high voltage gain converters suffer from complex control strategies and high cost due to the increased number of components. The quadratic boost converter is an interesting topology which uses a single active switch where the voltage ratio is given as a quadratic function of the duty ratio and it can be considered as a low cost and efficient solution for achieving a high voltage gain in PV applications with simple and conventional control strategies [10 –12]. For the monitor the quadratic boost converter, there is several MPPT control method. In generally, an MPPT fuzzy logic controller has better tracking performances compared with other algorithms [13, 14] such as the perturb and observer (P&O).

On the other hand, in order to achieve a good performance grid-connected photovoltaic (PV) system with low total harmonic distortion (THD), an adequate control of the voltage source inverter (VSI) is necessary. In high-power grid connected applications, three-phase inverters are preferred due to several advantages such as low current stress and higher efficiency. There are several control methods that

have been proposed in recent years for this type of inverters. The voltage oriented control (VOC) is a well-known method of controlling the three-phase VSI and it is based on current vector orientation with respect to the line voltage vector [15]. The VOC guarantees good static and dynamic performances via internal current control loops [15, 16]. However, this method presents some disadvantages such as coordinate transformation and a decoupling between active and reactive components is required [17]. The direct power control (DPC) is another control technique inspired from the principle of direct torque control (DTC) of AC machines [16]. In this control strategy, there are no internal current control loops, no PWM modulator block and the converter switching states are appropriately selected by a switching table based on the instantaneous errors between the commanded and estimated values of active and reactive power [15, 16]. The main disadvantage of the DPC is the high sampling frequency required to obtain satisfactory performance and the variable switching frequency, which generates an undesired harmonic components [18].

In this study, a predictive DPC (P-DPC) is performed by replacing the switching table and the hysteresis controllers in the conventional DPC by a predictive controller. The principle of the P-DPC control is based on the selection of the optimum control vector from the possible vectors to be applied during the sampling period. The selection is carried out by optimizing a suitable cost function in order to get a sinusoidal current and to ensure a good convergence of the active and reactive power to their references. The reminder of this paper is organized as follows. Section II presents the system description and the predictive DPC. Section III presents the model of the quadratic boost converter used as an interface between the PV generator and the VSI. Its control strategy based on a fuzzy logic approach to operate the system at its MPP is presented in Section IV. Numerical simulations are presented and discussed in Section V. Finally some concluding remarks are drawn in the last section.

2. System description and predictive direct power control

The system considered in this study is depicted in Fig. 1. It consists of a PV source connected to a DC-DC quadratic boost converter performing a fuzzy logic maximum power point tracking (MPPT), and feeding a three-phase VSI. With the aim of controlling the active and the reactive powers to their desired values, a suitable control strategy must be used for the inverter. In this paper, a predictive direct power control (P-DPC) will be used. Fig. 2 shows the block diagram of the proposed predictive DPC together with a conventional DPC using a hysteresis loop and a switching table. As can be seen, the main difference is that, in the predictive version, the hysteresis loop and the switching table are replaced by an optimization block to minimize a cost function. The latter is evaluated, at each sampling time, for all possible voltage vectors, over a finite prediction horizon, to select the optimal control vector that results in the lowest cost function value [19–21]. In this work, only one-step prediction horizon is considered to avoid difficulties that may arise in experimental implementation.
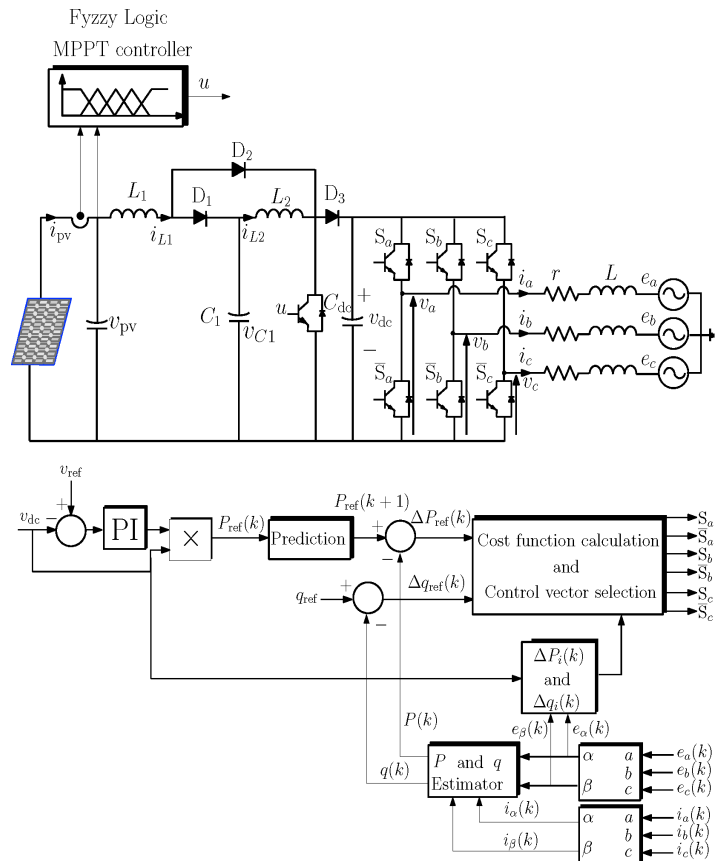

Fig 1. Schematic circuit diagram of a three-phase grid connected inverter supplied by a PV source through a quadratic boost converter performing the MPPT control.

However, the proposed control scheme can be easily expended to two-step prediction horizon using the cost function adopted in [22], which allows reducing the switching frequency and the power ripples. The sector, defined by the line voltage vector position θ, is also replaced by a block that calculates the active and reactive power difference.

Two sensors are usually required for this kind of control, one for the line voltage, and another one for the line current allowing the estimation of the instantaneous reactive and active powers Q and P according to the following equation:

$$\begin{cases} P = i_\alpha . e_\alpha + i_\beta . e_\beta \\ Q = i_\alpha . e_\beta - i_\beta . e_\alpha \end{cases} \tag{1}$$

By using Concordia transformation, the voltages $\left(e_\alpha, e_\beta\right)$ and the currents $\left(i_\alpha, i_\beta\right)$ in the $(\alpha\beta)$ frame are given by the following equations:

$$e_{\alpha\beta} = \begin{bmatrix} e_\alpha \\ e_\beta \end{bmatrix} = C_o \begin{bmatrix} e_a \\ e_b \\ e_c \end{bmatrix}, i_{\alpha\beta} = \begin{bmatrix} i_\alpha \\ i_\beta \end{bmatrix} = C_o \begin{bmatrix} i_a \\ i_b \\ i_c \end{bmatrix} \tag{2}$$

where the matrix C_o denotes Concordia transformation, and is given by

$$C_o = \sqrt{\frac{2}{3}} \begin{bmatrix} 1 & -\frac{1}{2} & -\frac{1}{2} \\ 0 & \frac{\sqrt{3}}{2} & -\frac{\sqrt{3}}{2} \end{bmatrix} \qquad (3)$$

The desired value Q_{ref} of the reactive power is given directly as null reference, and the active power reference P_{ref} is usually provided by a dc-bus voltage PI control block. In the conventional DPC, shown in Fig. 2(a), the errors between these references and their corresponding estimated values P and Q are applied to the hysteresis comparators whose outputs provide the signals u_p and u_Q, which can be equal to 0 or 1, depending on the tracking error. The voltage commands $e_{\alpha ref}$ and $e_{\beta ref}$ are selected based on a predefined table that uses the controller hysteresis outputs, and the line voltage vector position θ_n, given by

$$\theta_n = \arctan\left[\frac{e_\beta}{e_\alpha}\right] \qquad (4)$$
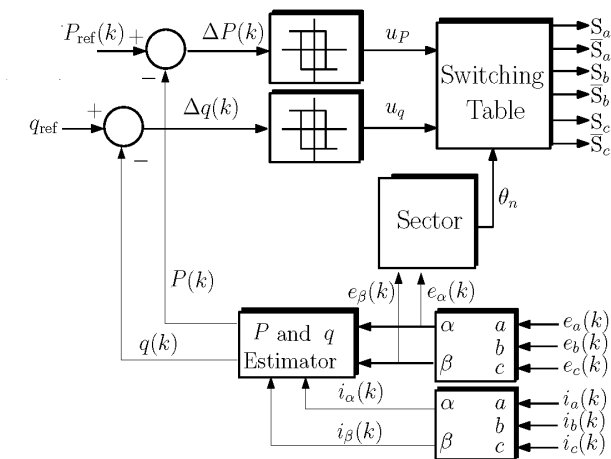
(a)
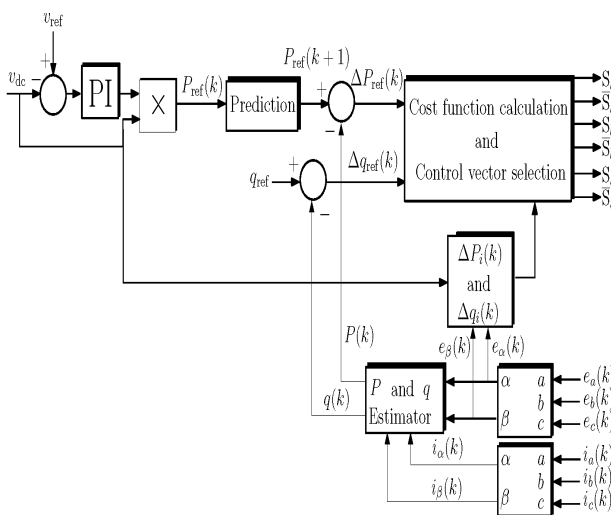
(b)

Fig 2. Block diagram of direct power control. (a) Conventional (b) predictive.

The switching states of the high side and the low side switches of the three-phase VSI can be readily determined based on the selected voltage commands. A look at the literature reveals that there are many tables that have been proposed with the aim of reducing the current ripples caused by the band-band controller, e.g., [18].

As mentioned before, in this paper, a minimization of a cost function is adopted to derive the predictive controller, as it was depicted in Fig. 2(b). It is noted that, unlike the existing predictive direct power control [19–22], the cost function is based on the change of active and reactive powers as follows

$$F_i = \min\left[\left(\Delta P^*(k) - \Delta P_i(k)\right)^2 + \left(\Delta Q^*(k) - \Delta Q_i(k)\right)^2\right] \qquad (5)$$

$$i = 0,..,7$$

where $i = [0,....,7]$ to consider all possible voltage vectors for a three-phase two-level VSI. The change in active and reactive power commands, $P_{ref}(k)$ and $Q_{ref}(k)$ are determined as follows

$$\begin{bmatrix} \Delta P_{ref}(k) \\ \Delta Q_{ref}(k) \end{bmatrix} = \begin{bmatrix} P_{ref}(k+1) - P(k) \\ Q_{ref}(k+1) - Q(k) \end{bmatrix} \qquad (6)$$

where the references of the active and reactive powers at k+1 instant are given as follows

$$\begin{bmatrix} P_{ref}(k+1) \\ Q_{ref}(k+1) \end{bmatrix} = \begin{bmatrix} 2P_{ref}(k) - P_{ref}(k-1) \\ Q_{ref}(k) \end{bmatrix} \qquad (7)$$

The actual active and reactive powers, P(k) and Q(k), are estimated as a function of the measured voltage and the current of the electrical grid using (1)–(3).

The predictive DPC requires a mathematical model to predict the actual change in active and reactive powers, $\Delta P_i(k)$ and $\Delta Q_i(k)$ at k + 1 instant, so as minimize the cost function F. This can be obtained by following the same procedures, as in [16], developed for a three-phase PWM rectifier.

That is,

$$\begin{bmatrix} P_i(k) \\ Q_i(k) \end{bmatrix} = \begin{bmatrix} P(k+1) - P(k) \\ Q(k+1) - Q(k) \end{bmatrix}_{v_{i\alpha}, v_{i\beta}} =$$

$$- \frac{T_s}{L} \begin{bmatrix} e_\alpha(k) & e_\beta(k) \\ e_\beta(k) & -e_\alpha(k) \end{bmatrix} \cdot \begin{bmatrix} e_\alpha(k) - v_{i\alpha}(k) \\ e_\beta(k) - v_{i\beta}(k) \end{bmatrix} \qquad (8)$$

The above equality is based on the assumption that the grid voltage is constant over the sampling period. It is noted that $v_{i\alpha}$ and $v_{i\beta}$ are determined by

$$v_{i\alpha} + j v_{i\beta} = \begin{cases} \sqrt{\frac{2}{3}} v_{dc} e^{j(i-1)\frac{\pi}{3}}, i = 1,...,6 \\ 0, i = 0,7 \end{cases} \qquad (9)$$

3. Modelling of the quadratic boost converter

Although, many converter topologies can be used to connect the PV source to the input of the three-phase VSI and for performing the MPPT [23, 24], in applications where the PV voltage source is much lower than the intermediate DC link voltage, a quadratic boost constitutes a low cost and efficient solution for achieving a high voltage gain. Fig. 3 shows the circuit diagram of a quadratic boost converter. The model is obtained from differential equations following [25].

$$
\begin{cases}
\dfrac{di_{L1}}{dt} = \dfrac{V_{pv}}{L_1} - \dfrac{V_{C1}}{L_1}(1-u) \\[2mm]
\dfrac{di_{L2}}{dt} = \dfrac{V_{C1}}{L_2} - \dfrac{V_{Co}}{L_2}(1-u) \\[2mm]
\dfrac{dv_{C1}}{dt} = \dfrac{i_{L2}}{C_1} + \dfrac{i_{L1}}{C_1}(1-u)
\end{cases}
\tag{10}
$$

$$
\frac{dv_{Co}}{dt} = -\frac{V_{C2}}{RC_2} + \frac{i_{L2}}{C_2}(1-u) - \frac{i_o}{C_2}
\tag{11}
$$

where u is the command signal applied to the main switch of the converter. All the remaining variables and parameters that appear in (10)–(11) can be identified in Fig. 3. In steady state regime, the control variable u can be represented by the duty cycle D, which represents its average value. Such a manipulation yields the relation

$$
\frac{v_{C1}}{v_{pv}} = \frac{v_{Cdc}}{v_{C1}} = \frac{1}{1-D}
\tag{12}
$$

Which leads to the ideal static transfer function of the converter M (D) [23]

$$
M(D) = \left(\frac{v_{C1}}{v_{pv}}\right)\left(\frac{v_{Cdc}}{v_{C1}}\right) = \frac{1}{(1-D)^2}
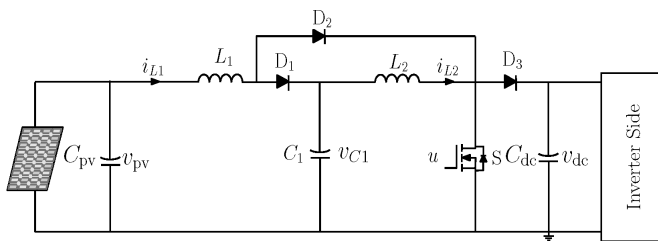\tag{13}
$$

Fig 3. Schematic block diagram of a quadratic boost converter.

4. Fuzzy logic MPPT controller

MPPT control plays a critical role in PV systems. The idea behind MPPT is to adjust the PV output power to it maximum value, which is mainly related to the changes in atmospheric conditions. A look at the literature reveals that there are different types of MPPT algorithms that can be used [26].

For instance, the perturb and observer (P&O) algorithm is the most commonly used MPPT controller because of the design simplicity. However, it is well-known that such a method suffers from the low convergence speed and the oscillation around the MPP, which raises concern about the choice of the step-size. To overcome these drawbacks, methods based on artificial intelligence such as fuzzy logic control [26] and artificial neural networks (ANN) techniques [27] have been recently proposed. Compared with other algorithms, the fuzzy logic control has better tracking performances [13, 14].

Namely, they have the advantage to be robust and relatively simple to design. The basic structure of a fuzzy controller is shown in Fig. 4.
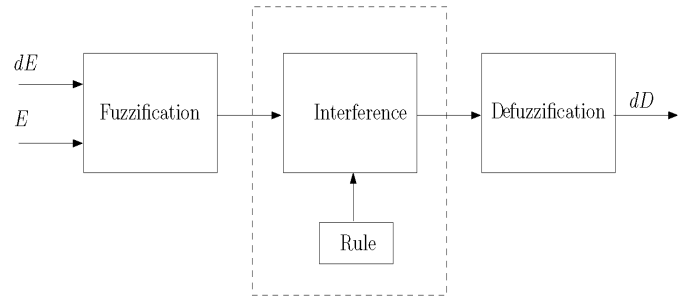

Fig .4. Basic structure of a fuzzy logic controller.

First, the two input variables, namely, the sampled values of the error E and change of error dE are calculated as follows:

$$
E(k) = \frac{P_{pv}(k) - P_{pv}(k-1)}{v_{pv}(k) - v_{pv}(k-1)}
\tag{14}
$$

$$
dE(k) = E(k) - E(k-1)
\tag{15}
$$

where $P_{pv}(k)$ and $v_{pv}(k)$ are, respectively, the power and the voltage of PV panel at sampling instants (kT_s). The input variable E(k) is used for determining if the estimated power at the instant kT_s is located on the left (E(k) > 0) or on the right (E(k) < 0) of the MPP of the PV characteristic [28], while the input variable dE(k) is used for determining the sign of the fuzzy logic perturbation [28]. Five linguistic variables are adopted for each of the input/output variables.

These are: NB (Negative Big), and NS (Negative Small), Z (Zero), PS (Positive Small) and PB (Positive Big). The five basic fuzzy subsets for the input and the output variables are presented in Fig. 5. Table. 1 presents the rule table of the fuzzy logic controller. In this paper, we use Mamdani fuzzy inference method for computing a fuzzy output value. The defuzzification transforms this fuzzy output into a numeric value. The most used defuzzification method is the centre of gravity method [29].

Table 1. Table of fuzzy rules.

E \ dE	NB	NS	Z	PS	PB
NB	Z	Z	PB	PB	PB
NS	Z	Z	PS	PS	PS
Z	PS	Z	Z	Z	NS
PS	NS	NS	NS	Z	Z
PB	NB	NB	NB	Z	Z

Accordingly, the change of the duty cycle is determined by following equation

$$dD = \frac{\sum_{j=1}^{n} \mu(D_j) - D_j}{\sum_{j=1}^{n} \mu(D_j)} \qquad (15)$$

Finally, the duty cycle is determined by:

$$D(k) = D(k-1) + dD(k) \qquad (16)$$

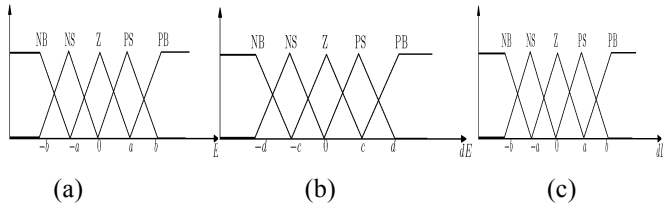(a)   (b)   (c)

Fig .5. Definitions and membership functions of (a) the first input variable (E), (b) the second input variable (dE) and (c) the output variable (dD).

5. Simulation results

Matlab Simulink with Simpower toolbox has been used for simulating the grid-connected PV system under the PDPC and supplied by a PV panel through a quadratic boost converter performing a fuzzy logic MPPT control described previously. The parameter values of the complete developed system are summarized in Table 2, 3, 4.

Table 2. Parameter of PV panel stp80

Rated Maximum Power P_{max}(W)	80
Maximum Power Voltage V_{mp}(V)	17.6
Maximum Power Current I_{mp} (A)	4.55
Open Circuit Voltage V_{oc} (V)	22.1
Short Circuit Current I_{sc} (A)	4.8

Table 3. Quadratic boost converter

Input Voltage (V)	17.6
Output Voltage (V)	400
Inductor L_1 (mH)	33
Inductor L_2 (mH)	33
Capacitor C_1 (µF)	100

Table 4. Parameters of electrical grid

Switching Period T_s (µs)	65
Resistance of Reactor r (Ω)	0.56
Inductance of Reactors L (mH)	19.5
DC-bus capacitor C_{dc} (µF)	1100
Source Voltage Frequency f (Hz)	50
DC-bus Voltage V_{dc} (µF)	400
Line to Line AC Voltage (V)	220

2.1. Static Performances

Fig. 6 shows the simulation results of the system under constant and nominal atmospheric conditions (temperature 25 C and irradiance 1000 W/m^2).
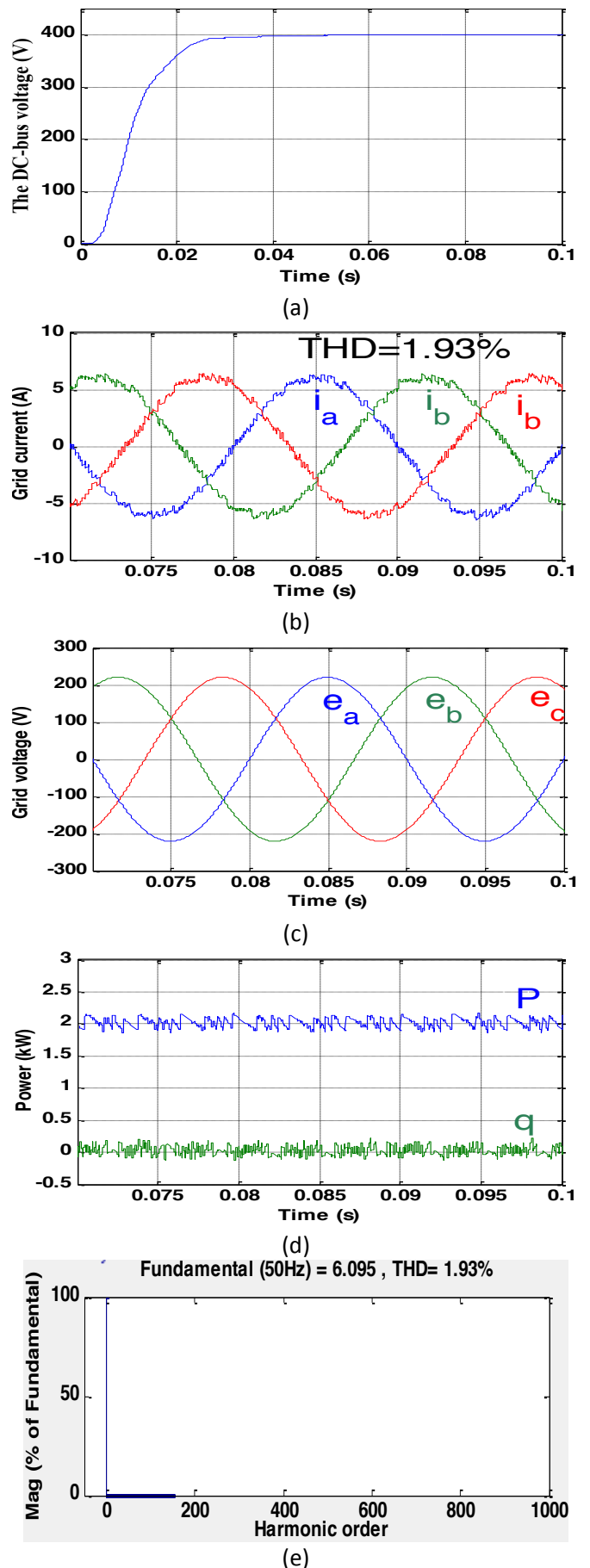

(a)

(b)

(c)

(d)

(e)

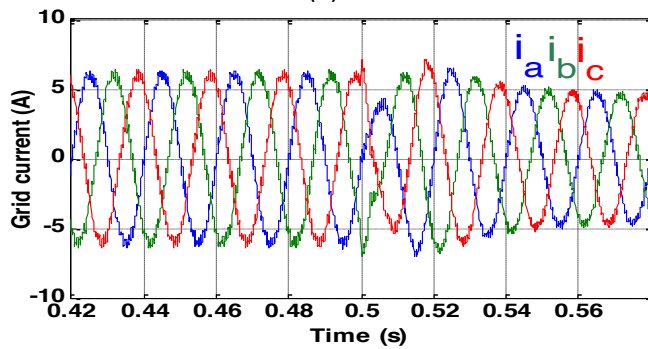**Fig .6.** Simulation results with constant of irradiance.

The DC bus voltage steady state value is reached in a relatively short time with negligible ripple oscillation in steady state, as is depicted in Fig. 6(a). The grid current and voltage are shown in Fig. 6.b and 6.c respectively, where it can be observed that both variables are synchronized and the power factor is close to unity. The grid phase current, waveforms are sinusoidal with a total harmonic distortion (THD) around 1.93%. The active and reactive powers of the grid are decoupled and are perfectly tracking their desired references. Note that the reactive power tends toward zero.

2.2. *Dynamic Performances*

In order to test the performance of this system under atmospheric condition changes, the system is simulated and the response of the system to step changes in the solar irradiation is obtained. It can be observed that the DC bus voltage tracks its reference with good accuracy as depicted in Fig. 7.a. Figs. 7.b and 7.c shows that the grid currents present very good tracking performances with a short transient time small harmonic distortion and that are in phase with the grid voltages.
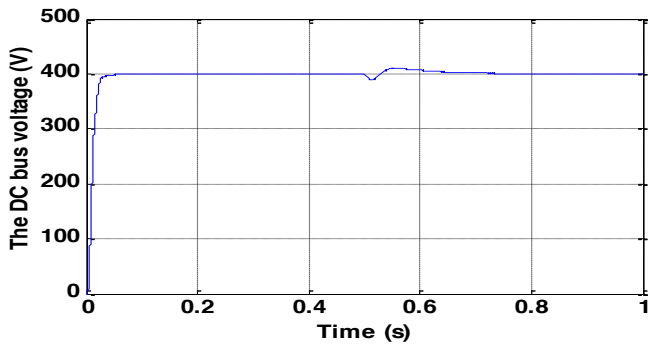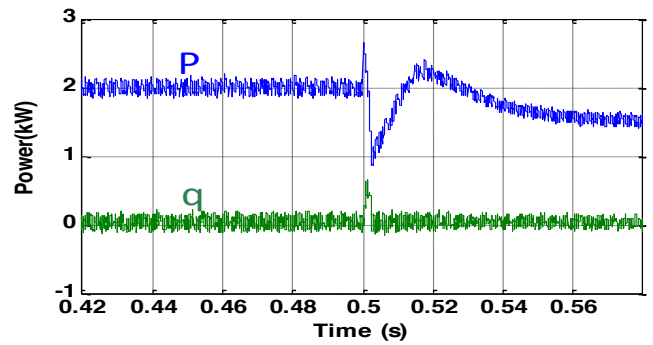

(a)

(b)
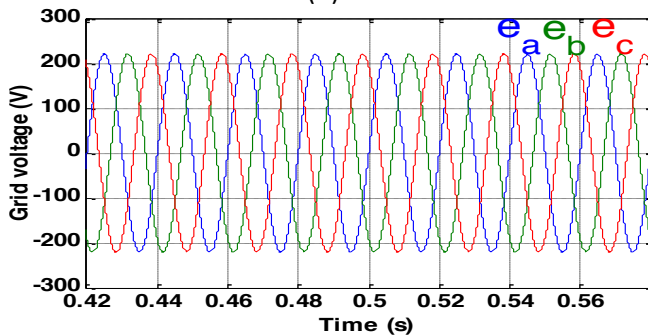
(c)

(d)

Fig .7. Simulation results with changes of irradiance. The change of irradiance at 0.5 s from 1000 W/m^2 to 800 W/m^2 with temperature at 25 C).

Finally, it can be observed in Fig 7.d that the active power properly follows their new references after a short transient, which confirms the robustness of the proposed solution. In addition, one can clearly see that the active and the reactive powers controls are decoupled of each other witch is one of the advantages of the used P-DPC.

6. Conclusion

In this study, we presented a predictive direct power control method for a two-stage grid-connected photovoltaic system. A quadratic boost converter is used as an interface performing an MPPT control and providing a high voltage gain which is suitable for PV applications. An artificial intelligence fuzzy logic based MPPT control was used giving a fast response in front of climatic changes and loading conditions. The good performances obtained by numerical simulations show the efficacy of predictive direct power control in PV systems.

References

[1] M. Orabi, M. Ahmed, and O. Abdel-Rahim, "A single-stage high boosting ratio converter for grid-connected photovoltaic systems," Electric Power Components and Systems, vol. 41, no. 9, pp. 896–911, 2013.

[2] M. Yue and X. Wang, "Assessing cloud transient impacts of solar and battery energy systems on grid inertial responses," Electric Power Components and Systems, vol. 43, no. 2, pp. 200–211, 2015.

[3] O. Abdel-Rahim and H. Funato, "A novel model predictive control for high gain switched inductor power conditioning system for photovoltaic applications," in Innovative Smart Grid Technologies-Asia (ISGT Asia),2014 IEEE. IEEE, 2014, pp. 170–174.

[4] A. Gandomkar and J.-K. Seok, "Inductive-boost switched-capacitor dc/dc converter for maximum power point tracking photovoltaic systems," in Energy Conversion Congress and Exposition (ECCE), 2014 IEEE. IEEE, 2014, pp. 5296–5303.

[5] K.-C. Tseng, C.-C. Huang, and W.-Y. Shih, "A high step-up converter with a voltage multiplier module for a

photovoltaic system," Power Electronics, IEEE Transactions on, vol. 28, no. 6, pp. 3047–3057, 2013.

[6] A. Alisson Alencar Freitas, F. Lessa Tofoli, E. Mineiro Sat' Jut'nior, S. Daher, and F. L. M. Antunes, "High-voltage gain DC–DC boost converter with coupled inductors for photovoltaic systems," Power Electronics, IET, vol. 8, no. 10, pp. 1885–1892, 2015.

[7] W. Li and X. He, "Review of nonisolated high-step-up dc/dc converters in photovoltaic grid-connected applications," Industrial Electronics, IEEE Transactions on, vol. 58, no. 4, pp. 1239–1250, 2011.

[8] R. Haroun, A. El Aroudi, A. Cid-Pastor, G. Garica, C. Olalla, and L. Martinez-Salamero, "Impedance matching in photovoltaic systems using cascaded boost converters and sliding-mode control," Power Electronics, IEEE Transactions on, vol. 30, no. 6, pp. 3185–3199, 2015.

[9] R. Haroun, A. Cid-Pastor, A. El Aroudi, and L. Martinez-Salamero, "Synthesis of canonical elements for power processing in DC distribution systems using cascaded converters and sliding-mode control," Power Electronics, IEEE Transactions on, vol. 29, no. 3, pp. 1366–1381, 2014.

[10] J. Morales-Saldana, R. Galarza-Quirino, J. Leyva-Ramos, E. Carbajal- Gutierrez, and M. Ortiz-Lopez, "Multi loop controller design for a quadratic boost converter," IET Electric Power Applications, vol. 1, no. 3, pp. 362–367, 2007.

[11] J. Leyva-Ramos, M. Ortiz-Lopez, L. Diaz-Saldierna, and J. Morales- Saldana, "Switching regulator using a quadratic boost converter for wide DC conversion ratios," IET Power Electronics, vol. 2, no. 5, pp. 605–613, 2009.

[12] O. López-Santos, L. Martínez-Salamero, G. Garcia, H. Valderrama- Blavi, and D. Mercuri, "Efficiency analysis of a sliding-mode controlled quadratic boost converter," Power Electronics, IET, vol. 6, no. 2, pp. 364–373, 2013.

[13] T. Radjai, L. Rahmani, S. Mekhilef, and J. P. Gaubert, "Implementation of a modified incremental conductance MPPT algorithm with direct control based on a fuzzy duty cycle change estimator using dspace," Solar Energy, vol. 110, pp. 325–337, 2014.

[14] T. Esram, P. L. Chapman et al., "Comparison of photovoltaic array maximum power point tracking techniques," IEEE Transactions on Energy Conversion EC, vol. 22, no. 2, pp. 439, 2007.

[15] M. Malinowski, M. P. Kazmierkowski, S. Hansen, F. Blaabjerg, and G. Marques, "Virtual-flux-based direct power control of three-phase PWM rectifiers," Industry Applications, IEEE Transactions on, vol. 37, no. 4, pp. 1019–1027, 2001.

[16] A. Bouafia, F. Krim, and J.-P. Gaubert, "Design and implementation of high performance direct power control of three-phase PWM rectifier, via fuzzy and PI controller for output voltage regulation," Energy Conversion and Management, vol. 50, no. 1, pp. 6–13, 2009.

[17] M. Malinowski, M. P. Kazmierkowski, and A. M. Trzynadlowski, "A comparative study of control techniques for PWM rectifiers in AC adjustable speed drives," Power Electronics, IEEE Transactions on, vol. 18, no. 6, pp. 1390–1396, 2003.

[18] A. Bouafia, J.-P. Gaubert, and F. Krim, "Predictive direct power control of three-phase pulse width modulation (PWM) rectifier using space-vector modulation (SVM)," Power Electronics, IEEE Transactions on, vol. 25, no. 1, pp. 228–236, 2010.

[19] D.-K. Choi and K.-B. Lee, "Dynamic performance improvement of AC/DC converter using model predictive direct power control with finite control set," Industrial Electronics, IEEE Transactions on, vol. 62, no. 2, pp. 757–767, 2015.

[20] P. Cortes, J. Rodríguez, P. Antoniewicz, and M. Kazmierkowski, "Direct power control of an afe using predictive control," Power Electronics, IEEE Transactions on, vol. 23, no. 5, pp. 2516–2523, 2008.

[21] J. Scoltock, T. Geyer, and U. K. Madawala, "Model predictive direct power control for a grid-connected converter with an LCL-filter," in Industrial Technology (ICIT), 2013 IEEE International Conference on. IEEE, 2013, pp. 588–593.

[22] J. Hu, J. Zhu, and D. G. Dorrell, "Model predictive control of grid connected inverters for PV systems with flexible power regulation and switching frequency reduction," Industry Applications, IEEE Transactions on, vol. 51, no. 1, pp. 587–594, 2015.

[23] N. Chettibi and A. Mellit, "Fpga-based real time simulation and control of grid-connected photovoltaic systems," Simulation Modelling Practice and Theory, vol. 43, pp. 34–53, 2014.

[24] N. Patcharaprakiti, S. Premrudeepreechacharn, and Y. Sriuthaisiriwong, "Maximum power point tracking using adaptive fuzzy logic control for grid-connected photovoltaic system," Renewable Energy, vol. 30, no. 11, pp. 1771–1788, 2005.

[25] O. Lopez-Santos, L. Martinez-Salamero, G. Garcia, H. Valderrama- Blavi, and T. Sierra-Polanco, "Robust sliding-mode control design for a voltage regulated quadratic boost converter," Power Electronics, IEEE Transactions on, vol. 30, no. 4, pp. 2313–2327, 2015.

[26] A. Gupta, S. Chanana, and T. Thakur, "Power quality assessment of a solar photovoltaic two-stage grid connected system: Using fuzzy and proportional integral controlled dynamic voltage restorer approach," Journal of Renewable and Sustainable Energy, vol. 7, no. 1, pp. 013113, 2015.

[27] Y.-H. Liu, C.-L. Liu, J.-W. Huang, and J.-H. Chen, "Neural-network based maximum power point tracking methods for photovoltaic systems operating under fast

changing environments," Solar Energy, vol. 89, pp. 42–53, 2013.

[28]   O. Guenounou, B. Dahhou, and F. Chabour, "Adaptive fuzzy controller based MPPT for photovoltaic systems," Energy Conversion and Management, vol. 78, pp. 843–850, 2014.

[29]   B. Bendib, F. Krim, H. Belmili, M. Almi, and S. Boulouma, "Advanced fuzzy MPPT controller for a stand-alone pv system," Energy Procedia, vol. 50, pp. 383–392, 2014.